Extreme anisotropy of wave propagation in two-dimensional photonic crystals

Yaroslav A. Urzhumov and Gennady Shvets
Department of Physics, The University of Texas at Austin, Austin, Texas 78712, USA
(Received 24 December 2004; revised manuscript received 20 May 2005; published 17 August 2005)

We demonstrate that electromagnetic waves propagating in square and hexagonal photonic crystals can have fundamentally different anisotropy properties. The wave frequency and group velocity can be functions of the propagation direction even for vanishingly small wave numbers (near the Γ-point). This anisotropy, present in square but absent in hexagonal lattices, can be so extreme that the group velocity can be either parallel or antiparallel to the phase velocity depending on the propagation direction. An analytic explanation of this effect based on the $\vec{k}\cdot\vec{p}$ perturbation theory and group-theoretical considerations is confirmed by electromagnetic simulations. One manifestation of the extreme anisotropy is the divergent van Hove singularity in the density of photonic states at the Γ-point. New applications, including surface-emitting quantum cascade lasers, are proposed.

DOI: 10.1103/PhysRevE.72.026608 PACS number(s): 42.70.Qs, 42.25.Bs, 42.55.Tv

Periodically arranged dielectric (and metallic) composites known as photonic crystals (PC's) have attracted a lot of interest in the past few years due to their ability to control electromagnetic (EM) wave propagation on and below the wavelength scale. PC's have found numerous applications in optics and optoelectronics [1]. Their unusual electromagnetic properties are derived from Bragg reflections giving rise to multiple propagation bands separated by the band gaps. It was realized early on that the symmetry points of zero group velocity at band edges can be exploited for various applications, including beam self-collimation [2], superprism effect [3], surface-emitting photonic crystal lasers [4,5], polarizers and wave plates [6], and negative refractive index [7–9]. Those points, which include the center (Γ-point) and the corners of the Brillouin zones, are characterized by high density of states, possibility of degeneracy, and, as we describe in this paper, nontrivial shapes of the equal frequency surface (EFS) in their vicinity.

The EFS concept is fundamentally important for predicting wave refraction at the PC interfaces [10]. We investigate the anomalies of wave propagation for small wave numbers $\vec{k}$, i.e., near the Γ-point (also often referred to as the center of the Brillouin zone). It is common to assume that, for $\vec{k}\to 0$, the EFS of a propagating EM wave in a highly symmetric (square or hexagonal) photonic crystal has a circular shape, making the wave propagation isotropic. This assumption follows from a simple mathematical fact: if the frequency ω is an analytic function of a small $\vec{k}$, then it must be expressible as $\omega^2=\omega_0^2+g_{mn}k_mk_n$. Because g_{nm} must be invariant with respect to the symmetry transformations of the crystal, the only option for the square or hexagonal lattices is $g_{mn}=C\delta_{mn}$, where C is a constant, and δ_{mn} is the Kronecker delta. The circular shape of the EFS has important consequences. For example, the phase and group velocities of the propagating waves are either parallel or antiparallel, depending on the sign of C. An elegant Hamiltonian optics description of wave propagation and refraction in PC's is also enabled [11].

Sufficiently far away from the Γ-point, EFS surfaces can, of course, become noncircular (e.g., elliptic, or even hyperbolic near the edges of the Brillouin zone [12]). The emphasis of this paper is on the properties of the EFS near the Γ-point. This point is not only special from the fundamental standpoint (small $\vec{k}$ expansion, for example, enables a ray optics description of light propagation in a photonic crystal with slowly varying parameters [13]), but also has important implications for surface-emitting devices. For example, the recently realized [5] surface emitting quantum cascade photonic crystal lasers were shown to lase at the frequency close to the center of the Brillouin zone.

We have found that if a propagation mode is doubly-degenerate at the Γ-point of the photonic dispersion curve, the EFS surface can be noncircular even for vanishingly small Bloch wave numbers. The anisotropy can be so strong that the angle between the phase and group velocities varies between 0 and 2π depending on the propagation directions. The resulting EFS has a hyperbolic shape near the Γ-point of the Brillouin zone. We refer to this strong anisotropy near the Γ-point as the *extreme anisotropy*. The noncircular EFS shape near the Γ-point has practical implications described towards the end of this paper. Whether such extreme anisotropy is indeed manifested is determined by the symmetry of the photonic crystal and its normal modes. We demonstrate that there is a crucial distinction between otherwise very similar square and hexagonal photonic crystal lattices; only the former can exhibit the extreme anisotropy.

In the remainder of this paper only TE modes [14] propagating in the (x,y) plane with the nonvanishing H_z, E_x, and E_y field components are considered. Very similar results can be obtained for the TM modes. The crystal is assumed infinite in the z-direction. The wave equation for the TE modes of a PC can be solved inside the unit cell of the lattice,

$$-\vec{\nabla}\cdot(\epsilon^{-1}(x,y)\vec{\nabla}H_z)=\frac{\omega^2}{c^2}H_z, \tag{1}$$

where H_z is subject to the periodic boundary conditions $H_z(\vec{r}+\vec{a})=H_z(\vec{r})e^{i\vec{k}\vec{r}}$, $\vec{a}$ is a vector connecting the opposite edges of the unit cell, and $\vec{k}$ is the Bloch wave number that belongs to the irreducible Brillouin zone [14]. The dielectric permittivity $\epsilon(x,y)$ is a periodic function defining the photo-

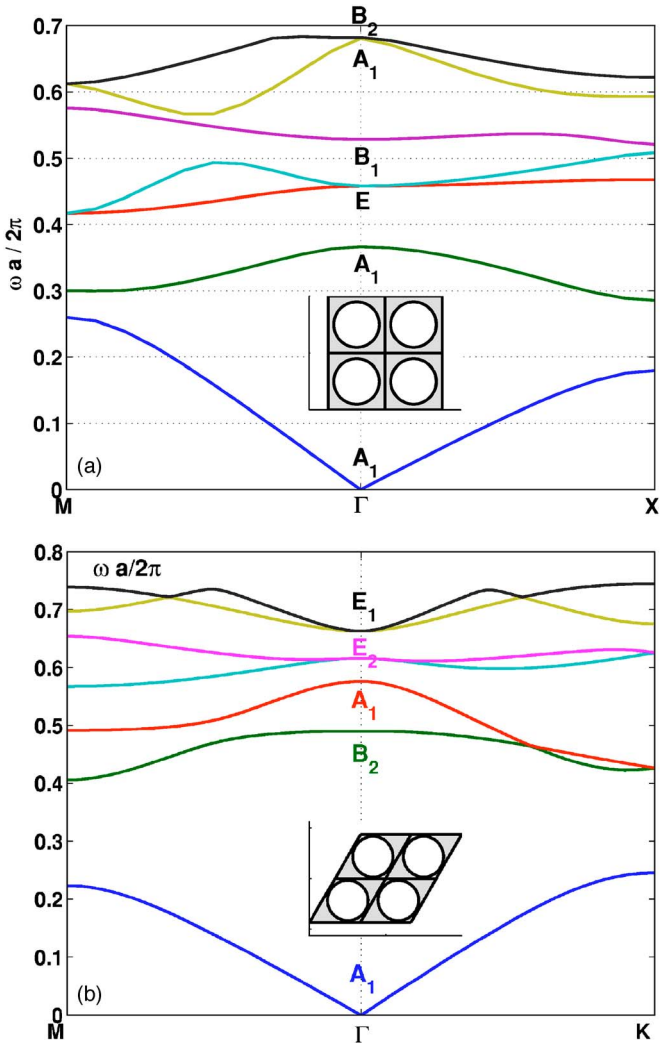

FIG. 1. (Color online) TE propagation bands $\omega(\vec{k})$ for the PC consisting of air holes of diameter $d=0.8a$ in silicon: (a) square lattice, and (b) hexagonal lattice. Four unit cells of each lattice are shown in the insets. Bands are labelled by their symmetry at the Γ-point. Band frequencies are scanned along the following directions inside the irreducible Brillouin zones: Γ-X $(0<\vec{k}<\vec{e}_x\pi/a)$ and Γ-M $(0<\vec{k}<(\vec{e}_x+\vec{e}_y)\pi/a)$ in (a), and Γ-M $(0<\vec{k}<2\vec{e}_y\pi/\sqrt{3}a)$ and Γ-K $(0<\vec{k}<4\pi\vec{e}_x/3a)$ in (b).

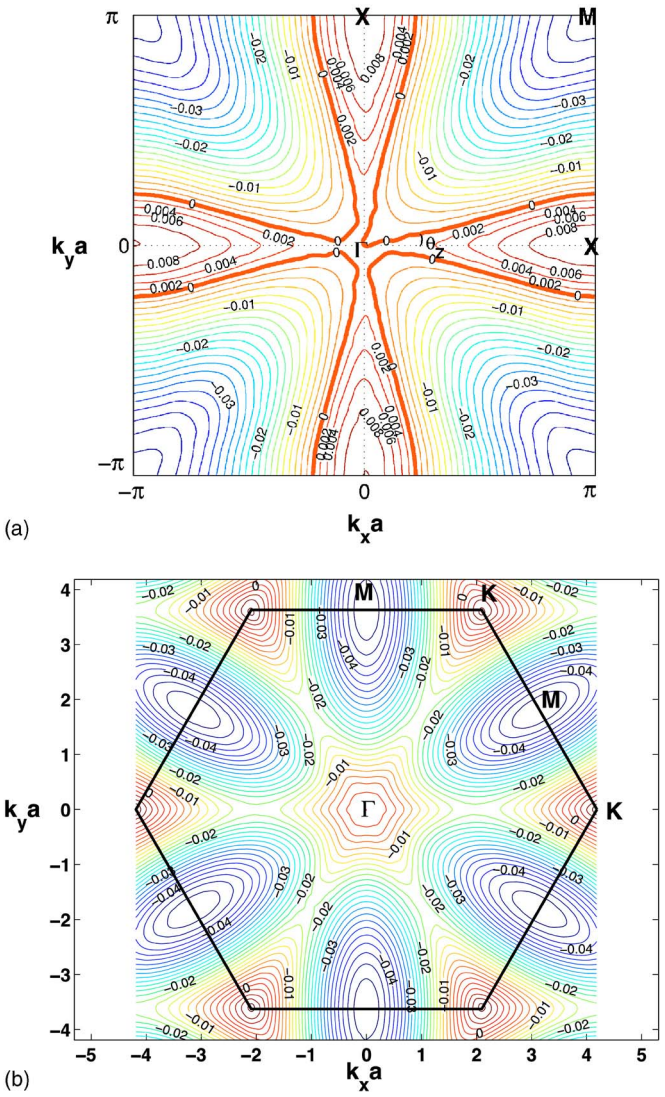

FIG. 2. (Color online) Equal frequency surfaces (EFS) for the lower-frequency branches of the degenerate at Γ-point bands: (a) the E-band of the square lattice, and (b) the E_2 band of the hexagonal lattice. Frequencies are labelled by $(\omega-\omega_0)a/2\pi c$, where $\omega_0=\omega(\vec{k}=0)$. For (a) $\omega_0 a/2\pi c=0.4587$, for (b) $\omega_0 a/2\pi c=0.6156$. Photonic crystal parameters: same as in Fig. 1.

nic crystal lattice. Two types of lattices shown in the insets in Fig. 1 were considered: a square and a hexagonal arrays of air holes in silicon ($\epsilon_{\mathrm{Si}}=12$) of diameter $d=0.8a$, where a is the lattice period. Numerical solution of Eq. (1) as an eigenvalue problem for $\lambda(\vec{k})\equiv\omega^2a^2/c^2$ using the finite elements code FEMLAB [15] yielded the dispersion curves $\omega(\vec{k})$ plotted in Fig. 1.

In addition to the Γ-point (GP), the other two high symmetry points shown in Fig. 1 are: X $(\vec{k}=\vec{e}_x\pi/a)$ and M $(\vec{k}=(\vec{e}_x+\vec{e}_y)\pi/a)$ for the square lattice shown in Fig. 2(a), and M $(\vec{k}=2\vec{e}_y\pi/\sqrt{3}a)$ and K $(\vec{k}=4\pi\vec{e}_x/3a)$ for the hexagonal lattice shown in Fig. 2(b). We labelled the multiple propagation bands according to their symmetry at the GP. The symmetries and degeneracies of the GP solutions are determined by the symmetry of $\epsilon(x,y)$. For example, the square lattice has a point group C_{4v} with five irreducible representations (IRREPS): four singlets (A_1,A_2,B_1,B_2), and one doublet E [16]. Consequently, only one- and twofold degeneracies in ω are present in a square lattice at the GP. Point group of a hexagonal lattice is C_{6v}, with the same singlet IRREPS as C_{4v} and two doublet IRREPS (E_1 and E_2).

The qualitative differences in the wave propagation near the GP for the two high-symmetry lattices are uncovered by plotting the EFS for the doubly-degenerate bands E and E_2 in Fig. 2. The EFS contours shown in Fig. 2 were obtained using the finite elements code FEMLAB [15]. In the vicinity of the GP the difference between the two lattices is striking: the hexagonal lattice has a circular EFS corresponding to isotropic wave propagation, whereas the square lattice has a hyperbolic EFS corresponding to strongly anisotropic propagation. For example, the frequency decreases away from the

Γ-point along the Γ-M direction and increases along the Γ-X direction. Therefore, the group and phase velocities are parallel along the principal directions of the lattice and antiparallel along the diagonal directions. The effective mass tensor of a photon $\partial^2\omega/\partial k_m \partial k_n$ has no definite sign; it depends on the propagation direction. The Brillouin zone is thus split into the regions of positive and negative $\omega(\vec{k})-\omega(\Gamma)$ by four $\omega(\vec{k})=\omega(\Gamma)$ curves shown as thick lines in Fig. 2(a), where $\omega(\Gamma)\equiv\omega_0$ is the frequency at the Γ-point. Noncircular equal frequency surfaces present intriguing implications for several applications, and also seem to be in contradiction with the simple analyticity argument presented earlier that implied $\omega^2=\omega_0^2+C\vec{k}^2$. Below we present a simple perturbation theory supporting the existence of the noncircular EFS. It is found that the frequency can become a nonanalytic function of $\vec{k}$ if it is degenerate at the Γ-point. We also note that the lengths of the isocontours $\omega(\vec{k})=\omega(\Gamma)$ are finite for the square lattice [shown in Fig. 2(a) as thick lines] and vanishing for the hexagonal lattice. As will be discussed below, this has important applications for the density of photonic states $S(\omega)$ in the vicinity of the Γ-point: $S(\omega)$ turns out logarithmically divergent for the square lattice and convergent for the hexagonal lattice.

The perturbation theory with respect to the Bloch wave number $\vec{k}$ is related to the $\mathbf{k}\cdot\mathbf{p}$ method in the electronic bands theory of solids [17]. It has been recently applied to the 2D [8,18] and 3D [19] photonic crystals. Magnetic field H_z is expressed as a Bloch wave: $H_z(x,y)=\psi(x,y)e^{i\vec{k}\vec{r}}$, where $\vec{r}=(x,y)$, $\vec{k}=(k_x,k_y)$, and ψ is a periodic function. Inserting H_z into Eq. (1) and introducing $\lambda\equiv\omega^2/c^2$, obtain an equation for ψ: $\mathcal{H}\psi(x,y)=\lambda\psi(x,y)$, where $\mathcal{H}$ is given by

$$\mathcal{H}(\vec{k})=-\vec{\nabla}\frac{1}{\epsilon}\vec{\nabla}-i\vec{k}\left(\frac{2}{\epsilon}\vec{\nabla}+\vec{\nabla}\frac{\epsilon}{\epsilon}\right)+\frac{k^2}{\epsilon}. \tag{2}$$

To apply the standard perturbation theory, first consider the unperturbed solutions of the eigenvalue equation $\mathcal{H}^{(0)}\psi_n^{(0)}=\lambda_n^{(0)}\psi_n^{(0)}$, where $\mathcal{H}^{(0)}=\mathcal{H}(\vec{k}=0)$ is the unperturbed Hamiltonian. Note that $\psi_n^{(0)}$ are the earlier discussed GP-solutions of the nth propagation band, their symmetry governed by the symmetry group of the PC. The perturbed $\vec{k}$-dependent solutions and the corresponding eigenvalues of the full wave equation $\mathcal{H}(\vec{k})\psi=\lambda_n(\vec{k})\psi$ are found by including the perturbation $\mathcal{V}=-i\vec{k}\cdot(2\epsilon^{-1}\vec{\nabla}+\vec{\nabla}\epsilon)+\vec{k}^2/\epsilon$.

For nondegenerate $\lambda_n^{(0)}$ (GP-solution is a singlet) the lowest-order perturbation theory yields [20]: $\lambda_n=\lambda_n^{(0)}+V_{nn}+\Sigma_{m\neq n}V_{nm}V_{mn}/(\lambda_n^{(0)}-\lambda_m^{(0)})+\cdots$, where the matrix elements of $\mathcal{V}$ are defined in the basis of GP functions: $V_{kl}=\int dx\int dy\,\psi_k^{(0)}\mathcal{V}\psi_l^{*(0)}$, with integration carried out over a unit cell. A singlet eigenvalue is thus an analytic function of the Cartesian components of the Bloch wave number k_x and k_y. The lowest order expansion in powers of k yields $\lambda(\vec{k})=\lambda^{(0)}+g_{mn}k_mk_n+\cdots$, where g_{mn} is a fully symmetric second rank tensor invariant with respect to the symmetry group of the crystal. Therefore, $g_{mn}=C\delta_{mn}$, and $\omega^2=\omega_0^2+C\vec{k}^2$ for all nondegenerate bands of the square and hexagonal lattices. We have numerically verified that the EFS of the A_1,A_2,B_1,B_2 bands shown in Fig. 1 are indeed circles. Note that the odd powers of $\vec{k}$ must vanish in the expansion of $\lambda=\omega^2/c^2$ because of the inversion symmetry of the considered hexagonal and square crystals.

For the degenerate $\lambda_n^{(0)}$ (GP-solution is a doublet) the *secular* perturbation theory [20] yields the $\lambda_n(\vec{k})$'s as the eigenvalues of the secular matrix W:

$$W_{nn'}=V_{nn'}+\sum_{m\neq n,m\neq n'}\frac{V_{nm}V_{mn'}}{\lambda_n^{(0)}-\lambda_m^{(0)}}+\cdots, \tag{3}$$

where $1\leqslant n,n'\leqslant 2$ for the doubly-degenerate band. Matrix elements V_{nm} (analogous to the transition amplitudes in quantum mechanics) connect the members of the doublet to each other as well as to the other bands. The perturbed eigenvalues λ are found by solving the equation $\lambda^2-(\mathrm{Tr}\,W)\lambda+\det W=0$, with the solutions

$$\lambda_\pm=\frac{\mathrm{Tr}\,W}{2}\pm\sqrt{\frac{(\mathrm{Tr}\,W)^2}{4}-\det W}. \tag{4}$$

Thus, λ (and the wave frequency) is a nonanalytic function of $\vec{k}$. Therefore, one cannot presume ω to be the function of $\vec{k}^2$ on the basis of its analyticity. Whether $\omega(\vec{k})$ is isotropic or anisotropic depends on whether the photonic crystal lattice is square or hexagonal. From Eq. (4) the eigenvalues can be expressed to the $O(k^2)$ order as $\lambda_\pm=P_2(k_x,k_y)\pm\sqrt{P_4(k_x,k_y)}$, where $P_n(k_x,k_y)$ are polynomials of order n in $\vec{k}$. The only invariant with respect to C_{4v} or C_{6v} symmetry groups second-order polynomial is $P_2(\vec{k})=k_x^2+k_y^2$. The difference between the hexagonal and square lattices appears in the invariant *fourth* order polynomials. For the hexagonal lattice the only such polynomial is the isotropic $P_4^{(1)}(\vec{k})=(k_x^2+k_y^2)^2$, whereas for the square lattice an anisotropic invariant polynomial exists: $P_4^{(2)}(\vec{k})=k_x^2k_y^2$. Therefore, for the hexagonal lattice we expect $\lambda_\pm=\alpha_1\vec{k}^2\pm\sqrt{\alpha_2\vec{k}^4}$ (fully isotropic), and for the square lattice $\lambda_\pm=\alpha_1k^2\pm\sqrt{\alpha_2k^4+\alpha_3k_x^2k_y^2}$ (in general, anisotropic), where α_{1-3} are constants.

The degree of anisotropy of a degenerate propagation band in a square lattice is determined by its nearby bands. As an example, consider the E-band shown in Fig. 1(a) known to be extremely anisotropic from Fig. 2(a). This can be analytically proven by keeping only the two closest bands A_1 and B_1 in Eq. (3). Contributions of the more distant in frequency bands are reduced by the $\lambda_{mn}^{(0)}\equiv\lambda_n^{(0)}-\lambda_m^{(0)}$ factor. We label the adjacent singlet levels 0 and 3, reserving the numbers 1, 2 for the degenerate band. Because $\mathrm{Tr}\,W=W_{11}+W_{22}$ is proportional to k^2 (isotropic), the isotropy or lack thereof is determined by that of $\det W$ according to Eq. (4). Because $\det W=-|\det Q|^2/\lambda_{10}^{(0)}\lambda_{31}^{(0)}$, where

$$Q=\begin{pmatrix}V_{10}V_{13}\\V_{20}V_{23}\end{pmatrix},$$

the doublet is anisotropic whenever $\det Q$ is an anisotropic polynomial. Properties of $\det Q$ depend on the symmetry properties of ψ_0 and ψ_3. It turns out that if the closest singlet levels are $A_{1,2}$ and $B_{1,2}$, then $\det Q$ is anisotropic. For other

level configurations det Q is either isotropic or zero. For our example of the E-band sandwiched between the two singlet bands A_1 and B_1 we find that $|\det Q|^2 \propto k_x^2 k_y^2$ resulting in anisotropy.

We have numerically calculated the dimensionless α-coefficients for the the E-doublet shown in Fig. 1(a) which are defined as

$$\frac{\omega^2}{c^2} = \alpha_1^2 |\vec{k}|^2 \pm (\alpha_2 |\vec{k}|^4 + \alpha_3 k_x^2 k_y^2)^{1/2}, \quad (5)$$

where the plus (minus) signs correspond to the upper (lower) doublet bands, respectively. All α's were found to be positive: $\alpha_1 = 0.212865$, $\alpha_2 = 0.01725$, $\alpha_3 = 0.7904$. Because $|\alpha_1 + \sqrt{\alpha_2}| \gg |\alpha_1 - \sqrt{\alpha_2}|$, the lower band supports much smaller group velocities along the principal axis than the upper band. Only the lower band of the E-doublet exhibit hyperbolic EFS in the vicinity of the Γ-point. We refer to the resulting anisotropy of the wave propagation as *extreme*. More precisely, anisotropy is referred to as extreme or moderate depending on whether the effective mass $\partial^2\omega/\partial k^2$ of a photon changes its sign as a function of the $\vec{k}$ direction or not. If it does not, the EFS are still convex (although not circular). That is the case for the upper frequency branch of the E doublet in Fig. 1. On the other hand, if $\partial^2\omega/\partial k^2$ changes sign, the EFS become hyperbolic and anisotropy extreme, as it is the case for the lower frequency branch of E shown in Fig. 2(a). Note that the hyperbolic nature of the EFS in the vicinity of the Γ-point can be deduced even from the band structure shown in Fig. 1(a): the frequency of the third doubly-degenerate band (labelled E) increases in the Γ-X direction and decreases in the Γ-M direction.

It is well known in the theory of solids [17] that nonanalyticity can lead to electron and hole mass anisotropy in the vicinity of band crossings, resulting in the constant energy surfaces shaped as "warped" spheres. However, anisotropy near the band minima (where it affects electron properties of a solid) is never strong enough to change the *sign* of the effective mass depending on the propagation direction. On the other hand, the extreme anisotropy in square lattice photonic crystals manifests itself in remarkable refractive properties as explained below.

Hyperbolic EFS near the GP has several remarkable consequences for wave refraction that, we speculate, could find useful applications in integrated optics. Consider a TE-polarized EM wave incident in the x-y plane at a small angle θ_{inc} with respect to the normal onto an air/PC interface. The interface is assumed normal to x-axis and the wave frequency $\omega_M < \omega < \omega_0$, so that only the lower (extremely anisotropic) branch of the E-band is excited for small θ_{inc}. For our specific example we chose $\omega_0 a/2\pi c = 0.4587$, $\omega_M a/2\pi c = 0.4170$, and $\omega a/2\pi c = 0.4580$. Propagation of the refracted into the PC wave can be determined [10] by the conservation of k_y. The normal to the EFS for a given k_y determines the group velocity inside the PC. In Fig. 3 we plot (solid line) the dependence of the group velocity angle in the crystal θ_{gr} vs the incidence angle θ_{inc}, both with respect to the normal. This dependence is unusual in two respects. First, there is a total reflection from the air/PC interface for *small* incidence angles $\theta < \theta_{\min} \approx 0.03$. The effect of small-angle total reflection cannot be realized for elliptic EFS, and can be used for designing novel low-group velocity waveguides. Second, for a range of small incidence angles $\theta_{\min} < \theta < \theta_{\max} \approx 0.25$ two distinct refracted waves propagate into the PC. The small-angle birefraction was confirmed by us by solving for a wave incident from air on a PC. In the inset in Fig. 3 we have plotted the cell-averaged y-component of the Poynting flux $\langle P_y \rangle$ of the refracted wave as the function of the depth x into the PC. Realistic for $\lambda = 0.75$ μm losses in Si were accounted for by using $\epsilon = 12 + 0.06i$. Diamonds correspond to the large incidence angle $\theta_{\text{inc}} = 0.4$. Only one wave is refracted and exponentially decays into the crystal. Smaller incidence angle $\theta_{\text{inc}} = 0.1$ results in two refracted waves as indicated by their beating (squares).

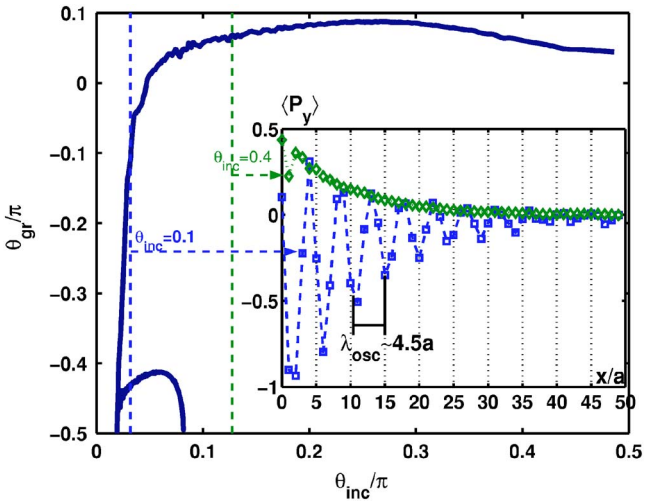

FIG. 3. (Color online) Refractive effects caused by the hyperbolic shape of the EFS at the frequency below the Γ-point ($\omega = 0.45802\pi c/a$) of a square PC. Crystal parameters: same as in Figs. 1 and 2. Main axes: group velocity angle of the refracted into PC wave(s) vs incidence angle. Inset: Cell-averaged Poynting flux $\langle P_y \rangle$ into the PC. Squares: small incidence angle $\theta_{\text{in}} = 0.1$ rad: two refracted waves are present and interfere (bi-refraction). Diamonds: large incidence angle $\theta_{\text{in}} = 0.4$ rad: single refracted wave.

Hyperbolic shape of the EFS can also be explored in designing directional surface-emitting photonic crystal (SEPC) lasers. SEPC quantum cascade lasers can be realized [5] by etching a two-dimensional array of holes through the laser active region. Vertical confinement is provided by the semiconductor and a metal film on top. A 2D PC simultaneously diffracts light vertically from the surface of the structure (out of the holes) and provides the in-plane confinement that is particularly strong near the high-symmetry points where v_g is small. Indeed, recent experiments [5] observed the highest optical power in the vicinity of the doubly degenerate Γ-point of a *hexagonal* PC. Directionality can then only be accomplished by shaping the PC cavity. Hexagonal crystals do not exhibit any anisotropy near the Γ-point as was shown below. They do, however, exhibit low group velocity near the Γ-point, and that is very advantageous for laser miniaturization. We suggest here that the square lattice SEPC laser may have advantages over its hexagonal lattice cousin. Specifi-

cally, the increased directionality of the in-plane band structure of a *square* lattice described in this paper may be used to emit light in a narrow range of angles from a SEPC laser. To see how in-plane dispersion relation determines the emission direction, consider EM fields in the holes on the surface of a laser oscillating with a relative phase shift determined by the in-plane Bloch wave numbers $\vec{k}$ excited in the 2D PC. The flux from the surface in the far field zone at the location $\vec{r}$ is proportional to the form-factor of the lattice, $F=\left|\sum_h e^{i(k_0\vec{n}_\parallel-\vec{k})\cdot\vec{r}_h}\right|^2$, where $k_0\equiv\omega/c$, $\vec{n}_\parallel=(\vec{r}-\vec{e}_z\cdot\vec{r})/r$, $\vec{r}_h$ are the positions of the holes on the surface, and the summation is over all holes. For a large PC $F\propto\delta^2(\vec{n}_\parallel-\vec{k}/k_0)$, which means that the horizontal direction of emission is controlled by the in-plane Bloch wave number $\vec{k}$.

If the gain has a maximum at the frequency slightly below $\omega(\Gamma)$, only the in-plane wave numbers in the four $\omega<\omega(\Gamma)$ triangles [circumscribed by the thick $\omega(\vec{k})=\omega(\Gamma)$ lines] shown in Fig. 2(a) are excited, and directional emission is accomplished. Moreover, the hyperbolic shape of the equal frequency surfaces dramatically increases the density of optical modes due to the Van Hove singularity [12], thereby increasing the spontaneous emission rate and the laser gain. This can be appreciated from the expression for the density of states [21] in a photonic crystal,

$$S(\omega)\propto\sum_m\int_{C(\omega_m)}\frac{dk_t}{v_g}, \tag{6}$$

where $C(\omega_m)$ is the EFS corresponding to $\omega=\omega_m$, the summation is carried over the index m labelling multiple disconnected EFS's corresponding to the same frequency, and k_t is the projection of $\vec{k}$ onto the tangent to the EFS $C_m\equiv C(\omega_m)$. Because in the vicinity of the Γ-point group velocity vanishes, the convergence or divergence of the density of states is determined by the length of the $C(\omega_m)$, L_m, in the limit of $\omega_m=\omega_\Gamma$. If L_m also vanishes for $\omega_m=\omega_\Gamma$ (as it is the case for concave/convex C_m's), then the density of states is finite. One example of a convex C_m is presented in Fig. 2(b) for a hexagonal photonic crystal. If L_m is finite, then the density of states diverges as $S(\omega)\propto\log[\omega(\Gamma)-\omega]$. For example, for the lower band of the E-doublet, C_m's for $\omega_m=\omega_\Gamma$ are shown in Fig. 2(a) as thick lines. Because those lines have finite lengths, the density of states is divergent.

In conclusion, we have demonstrated that electromagnetic wave propagation in the vicinity of the Γ-point can be extremely anisotropic in a square lattice two-dimensional photonic crystal. Extreme anisotropy occurs only in the propagation bands degenerate at the Γ-point. In our case this anisotropy also manifests itself in extremely low group velocity in the principal directions. The angle between the group and phase velocities in such a crystal varies between 0 and 2π. The shapes of the constant frequency surfaces of the extremely anisotropic propagation band are hyperbolic. One consequence of that is the logarithmic divergence of the density of states near the Γ-point. Possible applications include surface-emitting photonic crystal lasers that can be made more efficient and directional by the extreme anisotropy of the emitted electromagnetic waves.

This work is supported by the NSF's Nanoscale Exploratory Research Contract Nos. DMI-0304660 and the ARO MURI W911NF-04-01-0203.

[1] H. Benisty, S. Olivier, M. Rattier, and C. Weisbuch, in *Photonic Crystals and Light Localization in the 21st Century*, edited by C. M. Soukoulis (Kluwer Academic, Dordrecht, 2001).
[2] L. Wu, M. Mazilu, J.-F. Gallet, and T. F. Krauss, Photonics Nanostruct. Fundam. Appl. **1**, 31 (2003).
[3] H. Kosaka, T. Kawashima, A. Tomita, M. Notomi, T. Tamamura, T. Sato, and S. Kawakami, Phys. Rev. B **58**, R10096 (1998).
[4] M. Meier *et al.*, Appl. Phys. Lett. **74**, 7 (1999).
[5] R. Colombelli *et al.*, Science **302**, 1374 (2003).
[6] D. R. Solli, C. F. McCormick, R. Y. Chiao, and J. M. Hickmann, Appl. Phys. Lett. **89**, 1036 (2003).
[7] C. Luo, S. G. Johnson, J. D. Joannopoulos, and J. B. Pendry, Phys. Rev. B **65**, 201104(R) (2002).
[8] A. L. Efros and A. L. Pokrovsky, Solid State Commun. **129**, 643 (2004).
[9] G. Shvets and Y. Urzhumov, Phys. Rev. Lett. **93**, 243902 (2004).
[10] M. Notomi, Phys. Rev. B **62**, 10696 (2000).
[11] P. S. J. Russell and T. A. Birks, J. Lightwave Technol. **17**, 1982 (1999).
[12] A. Mekis, M. Meier, A. Dodabalapur, R. E. Slusher, and J. D. Joannopoulos, Appl. Phys. A: Mater. Sci. Process. **69**, 111 (1999).
[13] M. Onoda, S. Murakami, and N. Nagaosa, Phys. Rev. Lett. **93**, 083901 (2004).
[14] J. D. Joannopoulos, R. D. Meade, and J. N. Winn, *Photonic Crystals: Molding the Flow of Light* (Princeton University Press, Princeton, 1995).
[15] *FEMLAB Reference Manual, Comsol AB*, Stockholm, Sweden, version 2.2 ed. (2001).
[16] A. Haug, *Theoretical Solid State Physics* (Pergamon, Oxford, 1972).
[17] P. Y. Yu and M. Cardona, *Fundamentals of Semiconductors* (Springer-Verlag, Berlin, 1999).
[18] G. Shvets, Phys. Rev. B **67**, 035109 (2003).
[19] J. E. Sipe, Phys. Rev. E **62**(4), 5672 (2000).
[20] L. D. Landau and E. M. Lifshitz, *Quantum Mechanics* (Pergamon, London, 1991).
[21] R. C. McPhedran, L. C. Botten, J. McOrist, A. A. Asatryan, C. M. de Sterke, and N. A. Nicorovici, Phys. Rev. E **69**, 016609 (2004).